DOI: 10.1364/OE.25.010051

Research Article | Vol. 25, No. 9 | 1 May 2017 | OPTICS EXPRESS 10051
Optics EXPRESS

Structuring light under different polarization states within micrometer domains: exact analysis from the Maxwell equations

MICHEL ZAMBONI-RACHED,[1,*] LEONARDO ANDRÉ AMBROSIO,[2] AHMED H. DORRAH,[3] AND MO MOJAHEDI[3]

[1] *DECOM, FEEC, Universidade Estadual de Campinas (UNICAMP), Campinas, SP, Brazil*
[2] *SEL, São Carlos School of Engineering, University of São Paulo, São Carlos, SP, Brazil*
[3] *Department of Electrical and Computer Engineering at the University of Toronto, Toronto, ON, Canada*
[*] *mzamboni@decom.fee.unicamp.br*

Abstract: We show the possibility of arbitrary longitudinal spatial modeling of non-diffracting light beams over micrometric regions. The resulting beams, which are highly non-paraxial, possess subwavelength spots and can acquire multiple intensity peaks at predefined locations over regions that are few times larger than the wavelength. The formulation we present here provides exact solutions to the Maxwell's equations where the linear, radial, and azimuthal beam polarizations are all considered. Modeling the longitudinal intensity pattern at small scale can address many challenges in three-dimensional optical trapping and micromanipulation.

OCIS codes: (070.7345) Wave propagation; (260.2110) Electromagnetic optics.

References and links

1. H. E. Hernandez Figueroa, E. Recami, and Michel Zamboni-Rached, *Non-Diffracting Waves* (Wiley-VCH Verlag, 2014).
2. T. A. Planchon, L. Gao, D. E. Milkie, M. W. Davidson, J. A. Galbraith, C. G. Galbraith, and E. Betzig, "Rapid three-dimensional isotropic imaging of living cells using Bessel beam plane illumination," Nat. Methods **8**(5), 417–423 (2014).
3. D. G. Grier, "A revolution in optical manipulation," Nature **424**, 810–816 (2003).
4. M. Padgett and R. Bowman, "Tweezers with a twist," Nat. Photonics **5**(6), 343–348 (2011).
5. M. Zamboni-Rached, "Stationary optical wave fields with arbitrary longitudinal shape by superposing equal frequency Bessel beams: Frozen Waves," Opt. Express **12**(17), 4001–4006 (2004).
6. M. Zamboni-Rached and M. Mojahedi, "Shaping finite-energy diffraction-and attenuation-resistant beams through Bessel-Gauss beam superposition," Phys. Rev. A **92**, 043839 (2015).
7. M. Corato Zanarella and M. Zamboni-Rached, "Electromagnetic frozen waves with radial, azimuthal, linear, circular, and elliptical polarizations," Phys. Rev. A **94**, 053802 (2016).
8. T. A. Vieira, M. R. R. Gesualdi, and M. Zamboni-Rached, "Frozen waves: experimental generation," Opt. Lett. **37**(11), 2034–2036 (2012).
9. A. H. Dorrah, M. Zamboni-Rached, and M. Mojahedi, "Generating attenuation-resistant frozen waves in absorbing fluid," Opt. Lett. **41**(16), 3702–3705 (2015).
10. L. A. Ambrosio and M. Zamboni-Rached, "Analytical approach of ordinary frozen waves for optical trapping and micromanipulation," Appl. Opt. **54**(10), 2584–2593 (2015).
11. E. G. P. Pachon, M. Zamboni-Rached, A. H. Dorrah, M. Mojahedi, M. R. R. Gesualdi, and G. G. Cabrera, "Architecting new diffraction-resistant light structures and their possible applications in atom guidance," Opt. Express **24**(22), 25403–25408 (2016).
12. M. Zamboni-Rached and E. Recami, "Subluminal wave bullets: Exact localized subluminal solutions to the wave equations," Phys. Rev. A **77**, 033824 (2008).
13. R. L. Garay-Avendaño and M. Zamboni-Rached, "Exact analytic solutions of Maxwell's equations describing propagating nonparaxial electromagnetic beams," Appl. Opt. **53**, 4524-4531 (2014).

1. Introduction

A non-diffracting beam that has been recently utilized in many applications is the Bessel beam [1]. Despite their interesting diffraction-resistance and self-healing behavior, Bessel beams typically lack the high intensity gradient in their longitudinal direction, i.e., their longitudinal intensity

#287812 https://doi.org/10.1364/OE.25.010051
Journal © 2017 Received 1 Mar 2017; revised 2 Apr 2017; accepted 2 Apr 2017; published 24 Apr 2017

Optics EXPRESS

gradient is not sufficient to overcome the beam scattering force which is a critical requirement, for instance, in optical trapping. This drawback was mitigated by using a more advanced class of diffraction-resistant light beams, known as Frozen Waves (FWs) [5–7], whose longitudinal intensity profile can be made to follow a predefined pattern and thus possess a customized (strong) intensity gradient. FWs have been experimentally generated in several media [8, 9] and have been examined for possible applications in optical trapping [10, 11].

Previously, FW beams were obtained using discrete superposition of co-propagating Bessel beams. In this case, the longitudinal intensity profile was controlled over relatively large propagation distances (centimeters). In optical trapping and micromanipulation applications, however, it is desirable to shape the optical beam over micrometer space regions. This can be done more efficiently through a continuous superposition of Bessel beams which can be expressed as a discrete superposition of Mackinnon type beams [12]. However, longitudinal intensity control over small regions, few times larger than the wavelength, will result in highly non-paraxial beams. Accordingly, the previous scalar paraxial approximation of FWs breaks down and it becomes necessary to formulate the solution in an exact vectorial form of Maxwell's equations.

In this work, we extend the scalar method of FWs, based on continuous superposition of Bessel beams, to the vectorial case. Our formulation provides exact solutions of Maxwell's equations for structured light under different polarization states (linear, azimuthal, and radial) over micrometer space regions. In contrast with previous work [13] which also deals with non-paraxial beams via superposition of Mackinnon type beams, here we focus on beam spatial modeling.

We envision this generalized form of FWs to be useful for optical trapping purposes, where the achievable high intensity gradients can ensure three-dimensional optical trapping at predetermined points over micrometer regions. In addition, the results presented here can have significant impact on many other applications including nanofabrication, microlithography, imaging, super-resolution microscopy, plasmonic coupling and excitation, and magneto-optics.

2. Scalar method

An integral solution to the wave equation $\Box^2\Psi = 0$ in the case of azimuthal symmetry is given by a continuous superposition of zero-order Bessel beams over the longitudinal wavenumber k_z:

$$\Psi(\rho, z, t) \;=\; \exp(-i\omega t) \int_{-\omega/c}^{\omega/c} \mathrm{d}k_z \; S(k_z)\, J_0\left(\rho\sqrt{\frac{\omega^2}{c^2} - k_z^2}\right) \exp(ik_z z)\;, \tag{1}$$

It can be shown that by expanding $S(k_z)$ in a Fourier series, $S(k_z) = \sum_{n=-\infty}^{\infty} A_n \exp(in\frac{2\pi}{K}k_z)$, with $K = 2\omega/c$ and $A_n = F(-2n\pi/K)$, the exact solution of Eq.(1) is given by the following superposition of Mackinnon-type beams [12]

$$\Psi(\rho, z, t) \;=\; \exp(-i\omega t) \sum_{n=-\infty}^{\infty} F\left(-\frac{2n\pi}{K}\right) \mathrm{sinc}\left(\sqrt{\frac{\omega^2}{c^2}\,\rho^2 + \left(\frac{\omega}{c}\,z + n\pi\right)^2}\right), \tag{2}$$

which, as showed in [12], can present resistance to the diffraction effects, with a longitudinal intensity profile that can be chosen *a priori*, i.e., $|\Psi(\rho = 0, z, t)|^2 \approx |F(z)|^2$, where $F(z) = f(z)\, e^{iQz}$. Here, Q is a positive constant parameter that ensures that the spectrum $S(k_z)$ acquires negligible values for $k_z < 0$, yielding mostly forward-travelling Bessel beams in the superposition of Eq. (1). The spot radius, r_0, is related to Q through $r_0 \approx 2.4/\sqrt{\frac{\omega^2}{c^2} - Q^2}$.

We note that the beams given by Eq. (2) do not carry orbital angular momentum (OAM) as they are composed of zero order Bessel beams. However, this solution can be transformed into higher order solutions equivalent to considering a superposition of higher order Bessel beams. Starting with "0–th order" solution (2), an "ℓ order" solution can be obtained by applying the operator $U \equiv \exp(i\phi)\,[\partial/\partial\rho + (i/\rho)\partial/\partial\phi)]$ ℓ times. This provides an exact solution to the scalar wave

Optics EXPRESS

equation, resulting in beams carrying OAM of topological charge ℓ with a longitudinal intensity pattern similar to that of the "0–th order" solution, but shifted from $\rho = 0$ to a cylindrical surface with $\rho = \rho_\ell$. Here, ρ_ℓ is related to the parameter Q and can be approximately evaluated as the first non-null root of the equation $\left[\frac{d}{d\rho} J_\ell \left(\rho\sqrt{(\frac{\omega^2}{c^2} - Q^2)}\right)\right]_{\rho=\rho_\ell} = 0$.

While this scalar method is very effective for shaping the diffraction resistant beam within micrometer spatial regions, providing fast convergence for the series $\Psi(\rho, z, t)$ in Eq. (2), it cannot be used for our purpose of modeling the light beam over small regions (order of few wavelengths), without taking the vectorial nature of electromagnetic waves into account. Accordingly, in the following section, we extend the scalar method to the vectorial case in order to provide exact solutions to Maxwell's equations and generate beams whose longitudinal intensity can be modeled over micrometers.

3. Extending the method: vectorial beams

In this section, we obtain the vectorial beams as exact solutions of Maxwell's equations, shaping the longitudinal intensity profiles over micrometric regions. The extension of the scalar method to the vectorial case will be carried out directly through the electric and magnetic fields, while taking into account the cases of linear, azimuthal, and radial polarization. Naturally, any wavelength can be used. Here, in all examples, we will consider $\lambda = 0.532\mu$m, widely used in many applications.

3.1. Linear polarization

In this case, we consider the electric field as $\mathbf{E} = E_0 \Psi \hat{\mathbf{x}} + E_z \hat{\mathbf{z}}$, where E_0 is a constant with dimensions of electric field and Ψ is given by the solution in Eq. (2). The longitudinal component is given by the Gauss law (source free) $E_z = -E_0 \frac{\partial}{\partial x} \int \Psi \, dz$. From Eq. (1), we have that

$$\int \Psi \, dz = \exp(-i\omega t) \int_{-\omega/c}^{\omega/c} dk_z \, \frac{S(k_z)}{ik_z} J_0\left(\rho\sqrt{\frac{\omega^2}{c^2} - k_z^2}\right) \exp(ik_z z) \, . \tag{3}$$

The integral of Eq. (3) can be resolved as a superposition of Mackinnon type beams whose complex amplitudes are given by the Fourier coefficients of $S(k_z)/ik_z$ where, as we already know, $S(k_z) = \sum_{n=-\infty}^{\infty} F(-2n\pi/K) \exp(in\frac{2\pi}{K}k_z)$. In this way, it can be shown that

$$\frac{S(k_z)}{ik_z} = \frac{1}{K} \sum_{n=-\infty}^{\infty} g\left(-\frac{2n\pi}{K}\right) \exp(in\frac{2\pi}{K}k_z), \quad \text{where,} \quad g\left(-\frac{2n\pi}{K}\right) = \left[\int F(z) \, dz\right]_{z=-2n\pi/K} , \tag{4}$$

in such a way that

$$E_z = -E_0 \exp(-i\omega t) \cos\phi \sum_{n=-\infty}^{\infty} g\left(-\frac{2n\pi}{K}\right) \frac{\partial}{\partial\rho} \mathrm{sinc}\left(\sqrt{\frac{\omega^2}{c^2}\rho^2 + \left(\frac{\omega}{c} z + n\pi\right)^2}\right), \tag{5}$$

where we have used $\partial/\partial x = (\cos\phi)\,\partial/\partial\rho - (\sin\phi/\rho)\,\partial/\partial\phi$. We can thus model and shape the longitudinal intensity pattern of the linear transverse electric field component, $E_x = E_0\Psi$, through Eq. (2), taking into account that the axial field component will be given by Eq. (5). Furthermore, the corresponding magnetic field can be easily calculated from the Faraday law, where $\mathbf{B} = -\frac{i}{\omega}\left[\frac{\partial E_z}{\partial y}\hat{\mathbf{x}} + \left(\frac{\partial E_x}{\partial z} - \frac{\partial E_z}{\partial x}\right)\hat{\mathbf{y}} - \frac{\partial E_x}{\partial y}\hat{\mathbf{z}}\right]$.

As an example, we demonstrate a case in which we generate a linearly polarized light beam of spot radius $r_0 \approx 0.28$ μm with longitudinal intensity profile given by a super-Gaussian of depth 25.2 μm multiplied by an Airy function squared. For this, we choose $F(z)$ as

$$F(z) = \exp(iQz) \exp\left(-\frac{1}{2}\left(\frac{z}{Z}\right)^8\right) \mathrm{Ai}\left(3\pi\frac{\mathrm{z} - 0.8\mathrm{Z}}{\mathrm{Z}}\right). \tag{6}$$

Optics EXPRESS

Here, $Z = 12.61\ \mu$m and $Q = 0.7\omega/c$ (from $r_0 \approx 2.4/\sqrt{\frac{\omega^2}{c^2} - Q^2}$). As such, $E_x = E_0\,\Psi$, with Ψ given by Eq. (2). Figure 1(a) depicts the spectrum $S(k_z)$ in this case and Fig. 1(d) shows the longitudinal intensity $|F(z)|^2$, chosen for E_x, in the continuous blue line, and the result obtained through our solution of Eq. (2) in red dash line. A very good agreement is observed. In addition, the 3D intensity of the transverse beam component E_x is shown in Fig. 2(a). It is observed that the desired spatial modeling is successfully realized over microns scale. For this, we only used 105 terms in the series of Eq. (2). Finally, Fig. 2(b) shows the 3D intensity of the axial field component, E_z, given by Eqs. (5) and (4) and follows the same intensity profile of E_x.

3.2. Azimuthal polarization

In this subsection, we consider the case of azimuthal polarization with azimuthal symmetry, i.e., $\mathbf{E} = E_\phi(\rho, z, t)\,\hat{\boldsymbol{\phi}}$, where $E_\phi(\rho, z, t)$ must obey $\nabla^2 E_\phi - E_\phi/\rho^2 - \partial^2_{ct} E_\phi = 0$. A general propagating beam solution is given by an integral expression similar to Eq. (1), but with the "0–th" order Bessel function replaced with a first order one, that is

$$E_\phi(\rho, z, t) \;=\; \frac{c}{\omega}\, E_0\, \exp\left(-i\omega t\right) \int_{-\omega/c}^{\omega/c} \mathrm{d}k_z\; S'(k_z)\, J_1\left(\rho\sqrt{\frac{\omega^2}{c^2} - k_z^2}\right) \exp\left(ik_z z\right) . \tag{7}$$

Although it is possible to obtain an analytical solution to the integral appearing in Eq. (7) for any $S'(k_z)$, we adopt a simpler procedure by considering the derivative of Ψ, Eq. (2), with respect to ρ. This yields a superposition similar to Eq. (7), with $S'(k_z) = -\sqrt{\omega^2/c^2 - k_z^2}\, S(k_z)$. With this, the solution for E_ϕ becomes

$$E_\phi(\rho, z, t) \;=\; \frac{c}{\omega}\, E_0 \exp\left(-i\omega t\right) \sum_{n=-\infty}^{\infty} F\left(-\frac{2n\pi}{K}\right) \frac{\partial}{\partial\rho}\mathrm{sinc}\left(\sqrt{\frac{\omega^2}{c^2}\,\rho^2 + \left(\frac{\omega}{c}\,z + n\pi\right)^2}\right), \tag{8}$$

This solution preserves the desired longitudinal intensity pattern, $|F(z)|^2$, of the resulting beam, which is no longer concentrated along $\rho = 0$, but it is now concentrated over a cylindrical surface of radius ρ_1, which is approximately given by the first non-null root of the equation $\left[\frac{d}{d\rho} J_1\left(\rho\sqrt{(\frac{\omega^2}{c^2} - Q^2)}\right)\right]_{\rho=\rho_1} = 0$. The magnetic field $\mathbf{B}$ can be obtained from Faraday's law, which in this case provides $\mathbf{B} = B_\rho\,\hat{\boldsymbol{\rho}} + B_z\hat{\mathbf{z}}$. This results in

$$B_\rho(\rho, z, t) \;=\; \frac{ic}{\omega^2}\, E_0 \exp\left(-i\omega t\right) \sum_{n=-\infty}^{\infty} F\left(-\frac{2n\pi}{K}\right) \frac{\partial^2}{\partial z\partial\rho}\mathrm{sinc}\left(\sqrt{\frac{\omega^2}{c^2}\,\rho^2 + \left(\frac{\omega}{c}\,z + n\pi\right)^2}\right), \tag{9}$$

$$\text{and}\quad B_z(\rho, z, t) \;=\; -\frac{ic}{\omega^2}\, E_0 \exp\left(-i\omega t\right) \sum_{n=-\infty}^{\infty} F\left(-\frac{2n\pi}{K}\right) \frac{1}{\rho}\frac{\partial}{\partial\rho}\left[\rho\frac{\partial}{\partial\rho}\mathrm{sinc}\left(\sqrt{\frac{\omega^2}{c^2}\,\rho^2 + \left(\frac{\omega}{c}\,z + n\pi\right)^2}\right)\right], \tag{10}$$

As an example, we present a scenario in which we obtain azimuthally polarized light beam with a longitudinal intensity pattern given by two super-Gaussians of width 2.5μm, concentrated over a cylindrical surface of radius $\rho_1 \approx 0.24\mu$m, and separated by 5μm. In this case we choose

$$F(z) \;=\; \exp\left(iQz\right)\left[\exp\left(-\frac{1}{2}\left(\frac{z + Z/2}{Z/4}\right)^8\right) + \exp\left(-\frac{1}{2}\left(\frac{z - Z/2}{Z/4}\right)^8\right)\right] , \tag{11}$$

with $Z = 10\ \mu$m and $Q = 0.75\,\omega/c$. Our solution is then given by Eq. (8), where $F(z)$ is given by Eq. (11). In this case, only 77 terms in the series of Eq. (8) are sufficient to produce a very close result. Figure 1(b) shows the k_z spectrum $S'(k_z)$ whereas Fig. 1(e) depicts the predetermined longitudinal intensity pattern $|F(z)|^2$ chosen for E_ϕ (in continuous blue line). The result obtained

Optics EXPRESS

through the solution in Eq. (8) is shown in red dash line, exhibiting an excellent agreement. Figure 2(c) shows the 3D intensity of the electric field, E_ϕ, of the resulting beam.

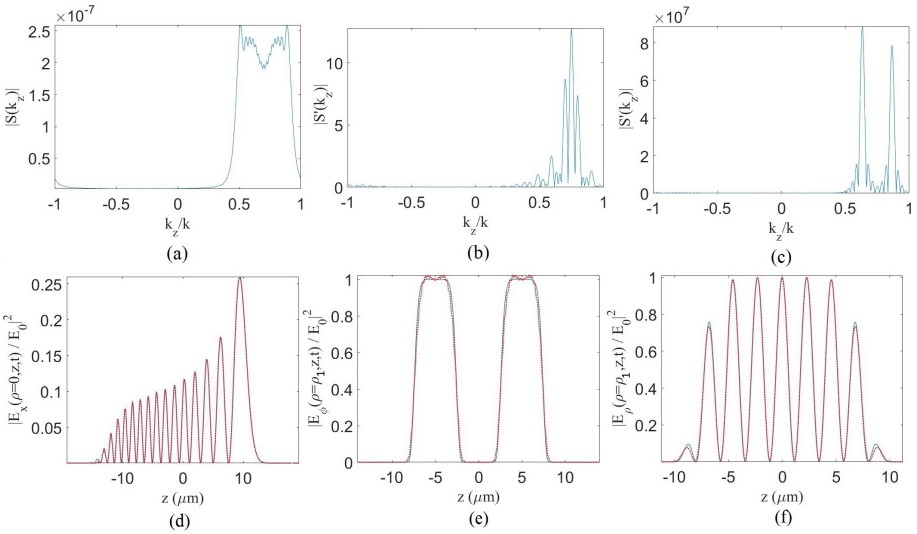

Fig. 1. The calculated spectra $S(k_z)$ and $S'(k_z)$ for the case of linear (a), radial (b), and azimuthal (c) polarization states. Figures (d-f) show the corresponding longitudinal intensity patterns, where the desired profile $|F(z)|^2$ is shown in the continuous blue line and the actual field profile in red dashed line exhibiting a very good agreement.

3.3. Radial polarization

Here, we derive the beam with radial polarization (E,B) from that with azimuthal polarization (E',B'). Using the concept of duality, we assign $E = cB'$ and $B = -1/cE'$ in $\mathbf{E}' = E'_\phi(\rho, z, t)\,\hat{\boldsymbol{\Phi}}$ and $\mathbf{B}' = B'_\rho\,\hat{\boldsymbol{\rho}} + B'_z\hat{\mathbf{z}}$. Accordingly, we obtain $\mathbf{E} = E_\rho\,\hat{\boldsymbol{\rho}} + E_z\hat{\mathbf{z}}$ and $\mathbf{B} = B_\phi(\rho, z, t)\,\hat{\boldsymbol{\Phi}}$ with

$$E_\rho(\rho,z,t) \;=\; \frac{ic^2}{\omega^2}\,E_0\exp\left(-i\omega t\right)\sum_{n=-\infty}^{\infty} F\left(-\frac{2n\pi}{K}\right)\frac{\partial^2}{\partial z\partial\rho}\mathrm{sinc}\left(\sqrt{\frac{\omega^2}{c^2}\,\rho^2+\left(\frac{\omega}{c}\,z+n\pi\right)^2}\right), \tag{12}$$

$$E_z(\rho,z,t) \;=\; -\frac{ic^2}{\omega^2}\,E_0\exp\left(-i\omega t\right)\sum_{n=-\infty}^{\infty} F\left(-\frac{2n\pi}{K}\right)\frac{1}{\rho}\frac{\partial}{\partial\rho}\left[\rho\frac{\partial}{\partial\rho}\mathrm{sinc}\left(\sqrt{\frac{\omega^2}{c^2}\,\rho^2+\left(\frac{\omega}{c}\,z+n\pi\right)^2}\right)\right], \tag{13}$$

$$\text{and}\qquad B_\phi(\rho,z,t) \;=\; -\frac{E_0}{\omega}\exp(-i\omega t)\sum_{n=-\infty}^{\infty} F\left(-\frac{2n\pi}{K}\right)\frac{\partial}{\partial\rho}\mathrm{sinc}\left(\sqrt{\frac{\omega^2}{c^2}\,\rho^2+\left(\frac{\omega}{c}\,z+n\pi\right)^2}\right). \tag{14}$$

As an example, we choose a field profile for E_ρ with intensity that is given by a sequence of seven donuts of radius $\rho_0 \approx 0.24\mu$m, with a longitudinal depth of 0.57μm and separated by a distance of 2.28μm. This can be obtained by choosing $|F(z)|^2$ as a cosine squared modulated by super-gaussian. More specifically, we choose

$$F(z) \;=\; \exp\left(iQz\right)\exp\left(-\frac{1}{2}\left(\frac{z}{Z}\right)^8\right)\cos\left(\frac{7\pi z}{2Z}\right), \tag{15}$$

with $Q = 0.75\,\omega/c$ and $Z = 8\mu$m. Figure 1(c) shows the k_z spectrum, $S'(k_z)$ whereas Fig. 1(f) shows the corresponding longitudinal intensity pattern $|F(z)|^2$ chosen for E_ρ in continuous blue

Optics EXPRESS

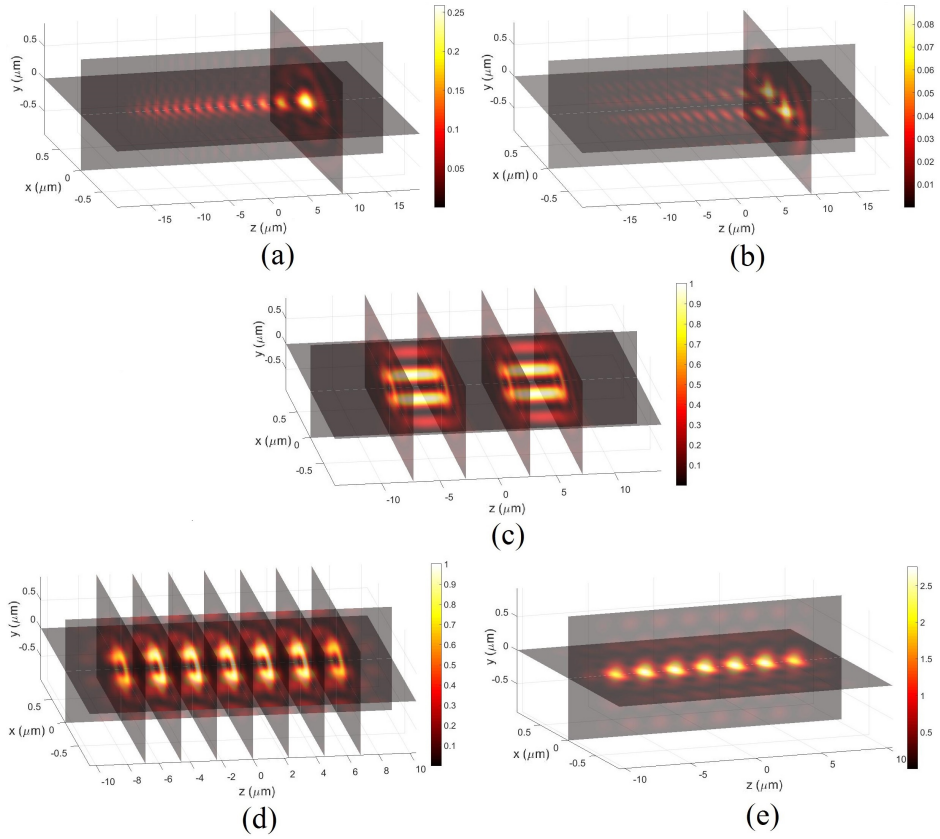

Fig. 2. The 3D intensities of: (a) E_x, for the case of linear polarization and (b) the corresponding axial field component E_z; (c) E_ϕ, for the azimuthal polarization; (d) E_ρ for the radial polarization and (e) the correspondent axial field component E_z.

line. The figure also depicts the result obtained via our solution from Eq. (12) in red dashed line. Figure 2(d) shows the 3D intensity of the transverse beam component E_ρ. In this case, we have incorporated 73 terms in the series of Eq. (2) to achieve the desired spatial modeling within the micrometer region. Finally, Fig. 2(e) shows the 3D intensity of the correspondent axial field component, E_z, given by Eq. (13), it follows the same longitudinal intensity pattern of E_ρ but possesses larger intensity as a result of the high non-paraxiality.

4. Conclusion

We presented the generalized Frozen Wave (FW) theory. Our formulation provides exact solutions to Maxwell's equations in which the three polarization states (linear, azimuthal, and radial) are considered. The method allows the generation of highly non-paraxial beams that can be spatially shaped over micrometer spatial regions, on demand. We envision this development to be useful for optical trapping and micro-manipulation purposes, nanofabrication, microlithography, imaging, super-resolution microscopy, plasmonic coupling and excitation, and magneto-optics.

Funding

Fundação de Amparo à Pesquisa do Estado de São Paulo (FAPESP) (2015/26444-8 and 2016/11174-8); Conselho Nacional de Desenvolvimento Científico e Tecnológico (CNPq) (304718/2016-5); Natural Sciences and Engineering Research Council of Canada (NSERC).